# miR-145 inhibits human non-small-cell lung cancer growth by dual-targeting RIOK2 and NOB1

KUN LIU[1], HONGLIN CHEN[2], QINGSHENG YOU[1], QING YE[3], FEI WANG[1], SHUO WANG[1],
SHUANGLONG ZHANG[1], KANGJUN YU[1], WEINAN LI[1] and MINGMING GU[1]

[1]Department of Cardiothoracic Surgery, Affiliated Hospital of Nantong University;
[2]School of Nursing, Nantong University; [3]Department of Obstetrics and Gynecology,
Affiliated Hospital of Nantong University, Nantong, Jiangsu 226001, P.R. China

**Abstract.** Non-small cell lung cancer (NSCLC) is a leading cause of cancer-associated mortality worldwide. Right open reading frame kinase 2 (RIOK2) and nin one binding protein (NOB1) are important accessory factors in ribosome assembly. In our previous study, RIOK2 and NOB1 were revealed to be highly expressed in NSCLC, and were associated with the clinicopathological characteristics of patients with NSCLC, i.e. TNM clinical stage, lymph node metastasis and differentiation. In addition, RIOK2 expression was correlated with NOB1. To further explore the mechanism and the RIOK2 and NOB1 signaling pathway, microRNA (miR) regulation was analyzed. The tumor suppressor miR-145 has been reported to be lowly expressed in numerous types of human cancer; in the present study, the expression levels of miR-145 were decreased in patients with NSCLC. Furthermore, RIOK2 and NOB1 were predicted to be the direct targets of miR-145 using bioinformatics software; this was further validated using a dual luciferase reporter assay. In addition, the protein expression levels of RIOK2 and NOB1 were inhibited in response to miR-145 overexpression, thus resulting in the suppression of cell viability, migration and invasion. These results suggested that RIOK2 and NOB1 may be potential targets in the treatment of NSCLC, and miR-145 may be considered a therapeutic inhibitor of both genes.

## Introduction

Non-small cell lung cancer (NSCLC) is the most common type of human lung cancer, which is associated with high mortality and accounts for ~90% of lung cancer cases (1). Due to its high mortality, there is a lack of effective treatments for NSCLC and the 5-year survival rate is very low. At present, the pathogenesis of NSCLC remains unclear; therefore, it is important to identify potential therapeutic targets.

Nin one binding protein (NOB1) is a subunit of the 19S regulatory particle of the 26S proteasome, which serves a crucial role in protease function and RNA metabolism (2). Our previous studies demonstrated that NOB1 is overexpressed in NSCLC and is associated with TNM stage, lymph node metastasis and histopathological grade (3,4). Right open reading frame kinase 2 (RIOK2) is a member of the RIO family (5), which has key roles in synthesis of the 40S ribosomal subunit and is essential for processing of 20S pre-ribosomal RNA (rRNA) to mature 18S rRNA (6,7). The results of our previous study indicated that NOB1 and RIOK2 are highly expressed in the tumor tissues of patients with NSCLC, and their expression profiles were revealed to be significantly associated with clinicopathological parameters, including TNM clinical stage, lymph node metastasis and differentiation. RIOK2 expression was also reported to be correlated with NOB1. These results suggested that NOB1 and RIOK2 may be potential targets for NSCLC therapy (8).

MicroRNAs (miRNAs/miRs) are a class of endogenous short non-coding RNAs, which are ~22 nucleotides in length, that serve important regulatory roles by targeting mRNAs for cleavage or translational suppression in animals and plants (9,10). miRNAs have been reported as oncogenes or tumor suppressor genes, which regulate tumorigenesis and metastasis through targeting various genes that are abnormally expressed in cancer cells (11). As a tumor suppressive miRNA, miR-145 has been reported to be decreased in numerous types of human cancer, including pancreatic cancer (12), prostate cancer (13), cervical cancer (14), gastric cancer (15), oral cancer (16), colorectal cancer (17), breast cancer (18), bladder cancer (19) and melanoma (20). These previous studies have indicated that miR-145 may suppress the growth, migration and invasion of cancer cells, and inhibit tumorigenesis by targeting various genes that are abnormally expressed in tumors.

The present study aimed to explore the expression of miR-145 in NSCLC, and to investigate the regulatory effects of miR-145 on the expression of RIOK2 and NOB1.

## Materials and methods

*Patient specimens.* A total of 30 tumor tissues and paired adjacent non-tumor lung tissues were obtained from patients with NSCLC (sex: Male, n=25; female, n=5; age: <60 years, n=4; ≥60 years, n=26) who had undergone primary surgical NSCLC resection at the Affiliated Hospital of Nantong University (Nantong, China) between April 2012 and December 2015. After collection, the tissues were frozen at -80°C. The present study was approved by the Ethics Committee of the Affiliated Hospital of Nantong University, and all of the experiments were performed in accordance with the approved guidelines of the Affiliated Hospital of Nantong University. Written informed consent was obtained from each patient prior to study enrollment.

*Cell culture and transfection.* The human NSCLC cell lines A549, H1299, H1975 and H1650, the human lung cell line BEAS-2B, and 293 cells (all from Cell Center of Central South University, Changsha, China) were maintained in Dulbecco's modified Eagle's medium (DMEM; Thermo Fisher Scientific, Inc., Waltham, MA, USA) supplemented with 10% fetal bovine serum (FBS; Thermo Fisher Scientific, Inc.) at 37°C in a humidified incubator containing 5% $CO_2$. Human miR-145 mimics and small interfering (si)RNAs were transfected into A549 and H1299 cells ($5x10^3$ cells) using Lipofectamine® 3000 transfection reagent (Invitrogen; Thermo Fisher Scientific, Inc.) according to the manufacturer's protocol at a concentration of 50 nmol/l. A miR-145 sequence-scrambled RNA oligonucleotide was used as a miRNA negative control (miNC). miR-145 mimics, siRNAs and negative controls were designed and obtained from Biomics Biotechnologies Co., Ltd. (Nantong, China). The miRNA and siRNA sequences were as follows: miR-145 mimics sense, 5'-GUCCAGUUUUCCCAGGAAUC CCU-3' and antisense, 5'-AGGGAUUCCUGGGAAAACUG GAC-3'; miNC sense, 5'-GUACGGCUCUCACCUUCCAU AGU-3' and antisense, 5'-ACUAUGGAAGGUGAGAGCCG UAC-3'; RIOK2-targeted siRNA (siRIOK2) sense, 5'-CAA UCAAGCUUUAGAAGAAdTdT-3' and antisense, 5'-UUCU UCUAAAGCUUGAUUGdTdT-3'; and NOB1-targeted siRNA (siNOB1) sense, 5'-GGAACAAGACCCUGAAGAAdTdT-3' and antisense, 5'-UUCUUCAGGGUCUUGUUCCdTdT-3'. In addition, a siRNA with no homology with human genes was used as a siRNA negative control (siNC), the sequences of which were as follows: Sense 5'-UUCUCCGAACGUGUCACG UdTdT-3' and antisense 5'-ACGUGACACGUUCGGAGAA dTdT-3'.

*Reverse transcription-quantitative polymerase chain reaction (RT-qPCR).* Total RNA was extracted from tissues and cells using TRIzol® reagent (Invitrogen; Thermo Fisher Scientific, Inc.), whereas small RNA enriched with miRNAs was isolated using the mirPremier® microRNA Isolation kit (Sigma-Aldrich; Merck KGaA, Darmstadt, Germany); these kits were used according to the manufacturers' protocols. Stem-loop RT-qPCR was performed to detect miR-145 expression according to a method previously described by Chen *et al* (21) using EzQuick™ miR-145 qPCR Detection Primer Set (Biomics Biotechnologies Co., Ltd.) and SYBR Green I (Thermo Fisher Scientific, Inc.); U6 small RNA was used as

an internal control. RT-qPCR was conducted using the SuperScript® III Platinum® SYBR® Green One-Step RT-qPCR kit (Thermo Fisher Scientific, Inc.) according to the manufacturer's protocol. β-actin was used as an internal control. The thermocycling conditions were as follows: RT for 30 min at 42°C; initial denaturation at 95°C for 5 min, followed by 45 cycles of denaturation at 95°C for 20 sec, annealing at 55°C for 30 sec, and extension at 72°C for 30 sec. The relative expression levels were evaluated using the $2^{-\Delta\Delta Cq}$ method (22). The RT-qPCR primer sequences were designed as follows: RIOK2 forward, 5'-ACAACAGGCAAGATGGTCA-3' and reverse, 5'-GACGACAAGGCAATTAGATGAG-3'; NOB1 forward, 5'-ACATACCAGTTGGAAGCAGAG-3' and reverse, 5'-CAGGTTCTCAGGCTCACAAG-3'; β-actin forward, 5'-CCACACCTTCTACAATGAG-3' and reverse, 5'-ATAGC ACAGCCTGGATAG-3'; miR-145 forward, 5'-ACACTCCAG CTGGGGGTCCAGTTTTCCCAGGA-3' and reverse, 5'-GTG CAGGGTCCGAGGT-3'; and U6 forward, 5'-AACGCTTCA CGAATTTGCGT-3' and reverse, 5'-CTCGCTTCGGCAGC ACA-3'.

*Dual luciferase reporter (DLR) assay.* TargetScan online software (http://www.targetscan.org/) was used to predict the miR-145-binding sites of RIOK2 and NOB1. Subsequently, RIOK2 (accession no. NM_018343, 111-1,769 sites) and NOB1 (accession no. NM_014062, 59-1,297 sites) human cDNA sequences (obtained from National Center for Biotechnology Information GenBank; https://www.ncbi.nlm.nih.gov/genbank/) of the predicted miR-145-binding regions in RIOK2 and NOB1 mRNA were inserted into pGL3 vectors (Promega Corporation, Madison, WI, USA) to obtain the following DLR vectors: Wild-type (wt)-plasmid (p) RIOK2- or wt-pNOB1-3' untranslated region (UTR), which were used to evaluate miR-145 activity. In addition, mutant (mt)-pRIOK2- or mt-pNOB1-3'UTR vectors were constructed as negative controls, in which the miR-145-binding sites were scrambled. Briefly, $1x10^5$ 293 cells/well were plated in a 24-well plate and cultured for 24 h at 37°C in a humidified incubator containing 5% $CO_2$. Subsequently, to determine the effects of miR-145 on RIOK2 expression, 80 ng/well wt- or mt-pRIOK2-3'UTR and 50 nmol/l miR-145 mimics or miNC were cotransfected into 293 cells using Lipofectamine® 3000 transfection reagent (Invitrogen; Thermo Fisher Scientific, Inc.) at 37°C for 48 h. To observe the effects of miR-145 on NOB1 expression, wt- or mt-pNOB1-3'UTR and miR-145 mimics or miNC were cotransfected into 293 cells. pRL-TK (Promega Corporation) was cotransfected into cells of each group as an internal control. Firefly and *Renilla* luciferase activities were measured 48 h post-transfection using the DLR assay system (Promega Corporation) according to the manufacturer's protocol.

*Western blot analysis.* A549 and H1299 cells were seeded into 6-well plates and cultured for 24 h. Following cell transfection for 48 h, cells were collected and lysed in protein lysis and extraction buffer (Thermo Fisher Scientific, Inc.) on ice. The lysates were then centrifuged at 13,800 x g for 20 min at 4°C and the protein concentration was determined by bicinchoninic acid assay (Promega Corporation). Subsequently, proteins (50 μg) were separated by 10% SDS-PAGE and electroblotted onto polyvinylidene difluoride (PVDF) membranes (EMD
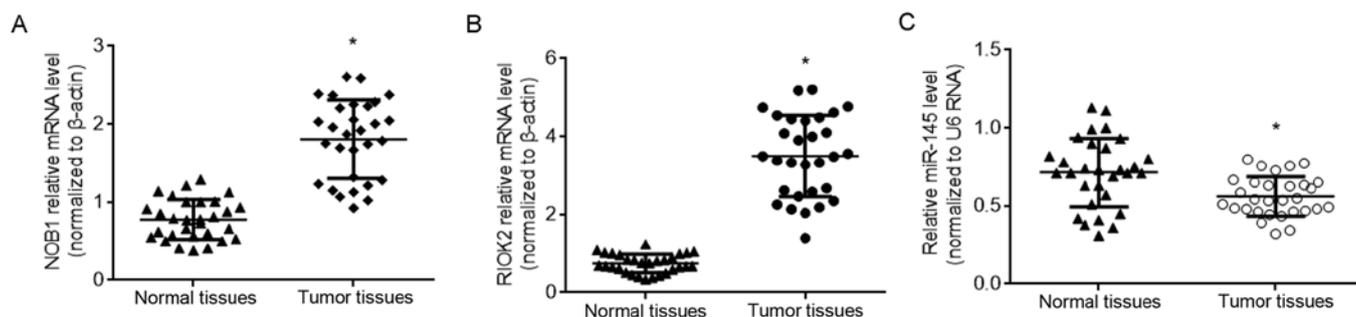
Figure 1. Expression levels of RIOK2, NOB1 and miR-145 in tumor tissues from patients with NSCLC, as detected by reverse transcription-quantitative polymerase chain reaction. mRNA expression levels of (A) RIOK2 and (B) NOB1 in NSCLC and non-tumor tissues. (C) Expression levels of miR-145 in NSCLC and non-tumor tissues. *P<0.05, compared with adjacent non-tumor lung tissues. miR-145, microRNA-145; NOB1, nin one binding protein; NSCLC, non-small cell lung cancer; RIOK2, right open reading frame kinase 2.

Millipore, Billerica, MA, USA). Subsequently, the membranes were blocked with 1% bovine serum albumin (Sangon Biotech Co., Ltd., Shanghai, China), and incubated with anti-RIOK2 (1:1,000; cat. no. ab172717), anti-NOB1 (1:1,000; cat. no. ab228985) and anti-β-actin antibodies (1:5,000; cat. no. ab8226) (all from Abcam, Cambridge, MA, USA). β-actin was used as an internal control. After washing with Tris-buffered saline with 0.1% Tween-20 (TBST), the PVDF membranes were incubated with the following horseradish peroxidase-conjugated secondary antibodies: Goat anti-mouse immunoglobulin (Ig)G (1:2,000; cat. no. ab205719) for RIOK2 and NOB1; goat anti-rabbit IgG (1:2,000; cat. no. ab205718) for β-actin (all from Abcam) for 1.5 h at room temperature. Finally, membranes were washed with TBST and the specific proteins were detected using an enhanced chemiluminescence substrate (Thermo Fisher Scientific, Inc.). The blots were semi-quantified using ImageJ (v1.45) software (National Institutes of Health, Bethesda, MD, USA).

*Cell viability assay.* An MTT Cell Viability Assay kit (Thermo Fisher Scientific, Inc.) was used to measure cell viability. Briefly, the cultured A549 and H1299 cells were plated into a 96-well plate at $5 \times 10^3$ cells/well and were grown to ~75% confluence over 24 h at 37˚C. Following transfection for 0, 24, 48, 72 and 96 h, the medium was removed and replaced with 100 $\mu$l fresh DMEM, and 10 $\mu$l 12 mmol/l MTT solution was added to each well. A negative control well containing 100 $\mu$l medium only was treated with 10 $\mu$l MTT solution. Following incubation at 37˚C for 4 h, 100 $\mu$l SDS-HCl (0.01 mol/l) solution was added to each well, mixed thoroughly and incubated at 37˚C for 4 h. Finally, each sample was mixed again and absorbance was measured at 570 nm using a microplate reader.

*Cell migration assay.* The Transwell assay was used to measure cell migration. Briefly, $1.5 \times 10^5$ A549 or H1299 cells/well were seeded into a 24-well plate and grown for 24 h. After transfection for 48 h, the cells were suspended in DMEM at a density of $1 \times 10^6$ cells/ml. The Transwell chambers (Corning Incorporated, Corning, NY, USA) were initially incubated with DMEM at 37˚C for 1 h; an 8-$\mu$m pore polycarbonate membrane separated the upper and lower chambers. Subsequently, 100 $\mu$l cell suspensions were added to the upper chamber, whereas 600 $\mu$l DMEM containing 10% FBS and conditioned medium (1:1 dilution) was added to the lower chamber. Conditioned

media were obtained from the cultures of A549 or H1299 cells, which were transfected with miR-145 or miNC for 48 h. Post-incubation for 24 h at 37˚C, the cells on the top surface of the membrane were carefully removed using a cotton swab, whereas cells on the bottom surface were fixed in 10% formaldehyde for 30 sec and stained with 0.5% crystal violet solution. After washing with PBS, the cells on the top surface of the membrane were carefully removed again. Cells on the bottom surface of the membrane were observed and counted under a microscope (Nikon 90i; Nikon Corporation, Tokyo, Japan).

*Cell invasion assay.* Cell invasion was detected using Transwell chambers coated with Matrigel. The assay was performed using the same protocol as for the cell migration assay, with the exception that the 8-$\mu$m pore polycarbonate membrane was coated with 50 $\mu$l 0.5 mg/ml Matrigel (BD Biosciences, Franklin Lakes, NJ, USA).

*Statistical analysis.* All experiments were performed independently at least three times. Data are presented as the means ± standard deviation. Statistical analyses were performed using SPSS 18.0 software (SPSS, Inc., Chicago, IL, USA); Spearman's correlation analysis was used to conduct correlations analyses. Significance between multiple groups was evaluated by one-way analysis of variance followed by a Dunnett post hoc test. Comparisons between two groups was performed by Student's t-test. All P-values are based on two-sided statistical analyses; P<0.05 was considered to indicate a statistically significant difference.

**Results**

*Expression levels of RIOK2, NOB1 and miR-145 in samples from patients with NSCLC.* The mRNA expression levels of RIOK2 and NOB1 were detected in 30 NSCLC tumor tissues and paired adjacent non-tumor lung tissues using RT-qPCR. The results demonstrated that the mRNA expression levels of RIOK2 and NOB1 were increased in tumor tissues compared with in non-tumor lung tissues (P<0.05; Fig. 1A and B). In addition, miR-145 expression was detected in tumor tissues by stem-loop RT-qPCR; the results indicated that the expression levels of miR-145 were decreased in tumor tissues compared with in non-tumor lung tissues (P<0.05; Fig. 1C). Spearman's
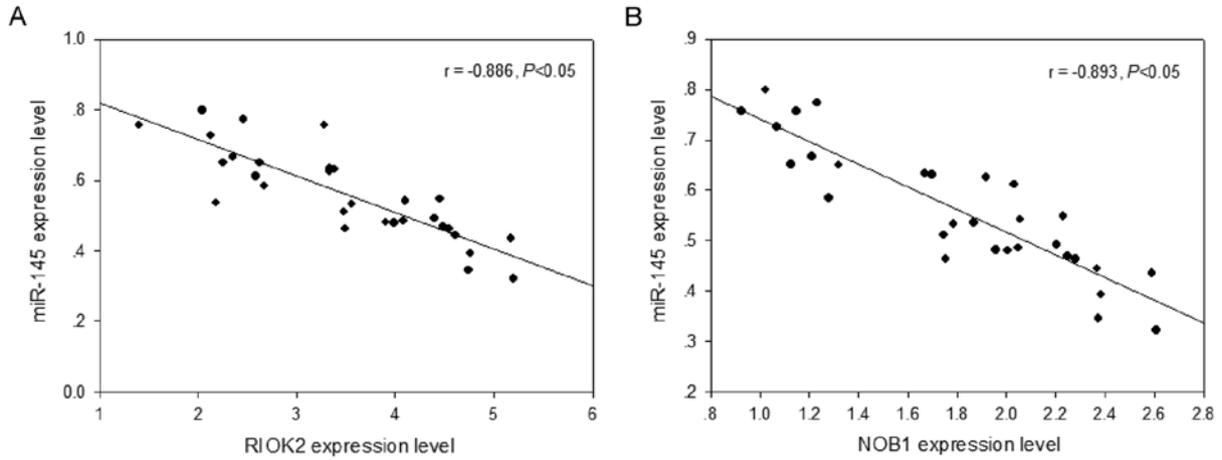
Figure 2. Correlation analysis. Correlation between (A) miR-145 and RIOK2, and (B) miR-145 and NOB1 expression in non-small cell lung cancer tissues. miR-145, microRNA-145; NOB1, nin one binding protein; RIOK2, right open reading frame kinase 2.
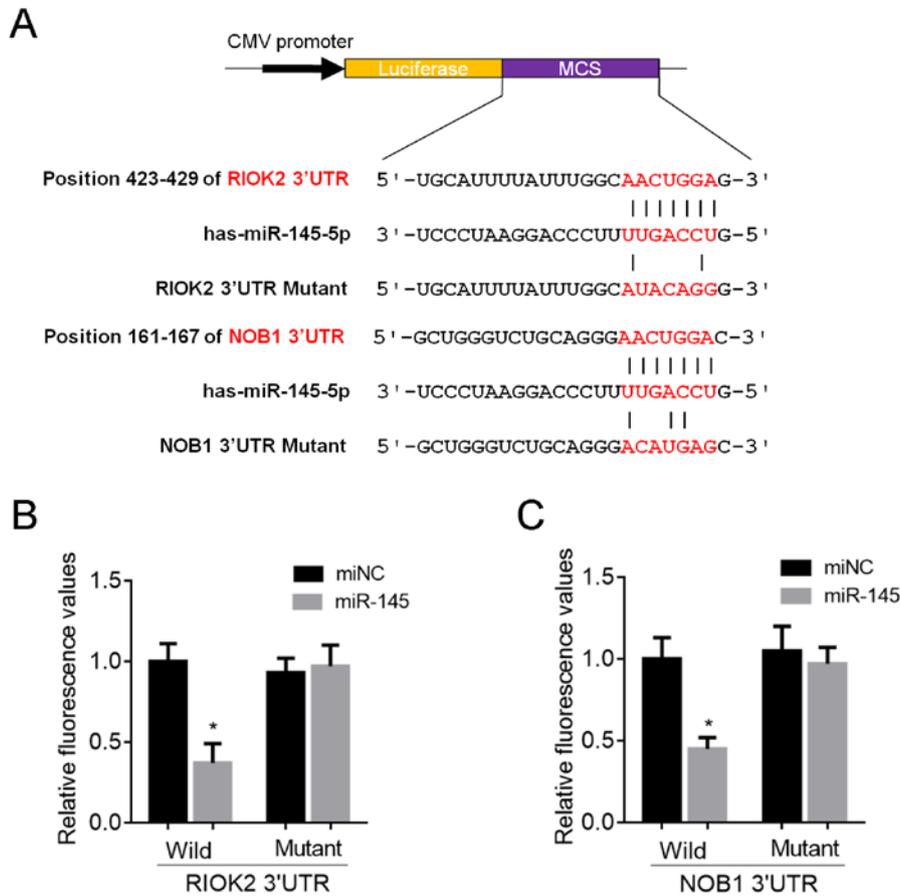


Figure 3. miR-145 targets the 3'UTR regions of RIOK2 and NOB1 mRNA. (A) As predicted by software, there was one binding site for miR-145 at position 423 of RIOK2 and position 161 of NOB1. The following DLR vectors were constructed: wt-RIOK2 or NOB1-3'UTR, and mutant-RIOK2 or NOB1-3'UTR. miR-145-induced inhibition of (B) RIOK2 and (C) NOB1 was detected by DLR assay. *P<0.05, compared with cells cotransfected with miNC and wt-RIOK2 or NOB1-3'UTR. 3'UTR, 3' untranslated region; DLR, dual luciferase reporter; miR-145, microRNA-145; miNC, miRNA negative control; NOB1, nin one binding protein; RIOK2, right open reading frame kinase 2; wt, wild-type.

correlation analysis revealed that miR-145 was negatively correlated with RIOK2 and NOB1 expression (RIOK2, r=-0.886, P<0.05; NOB1, r=-0.893, P<0.05) (Fig. 2).

*miR-145 targets the 3'UTR regions of RIOK2 and NOB1 mRNA.* As predicted by TargetScan online software, RIOK2

and NOB1 each possess a miR-145-binding site, at position 423 in RIOK2 mRNA and position 161 in NOB1 mRNA. The following DLR vectors: wt-RIOK2 or NOB1-3'UTR, and mt-RIOK2 or NOB1-3'UTR, were constructed in order to verify the inhibitory effects of miR-145 (Fig. 3A). Following cotransfection of 293 cells with miR-145 mimics and wt-RIOK2 or
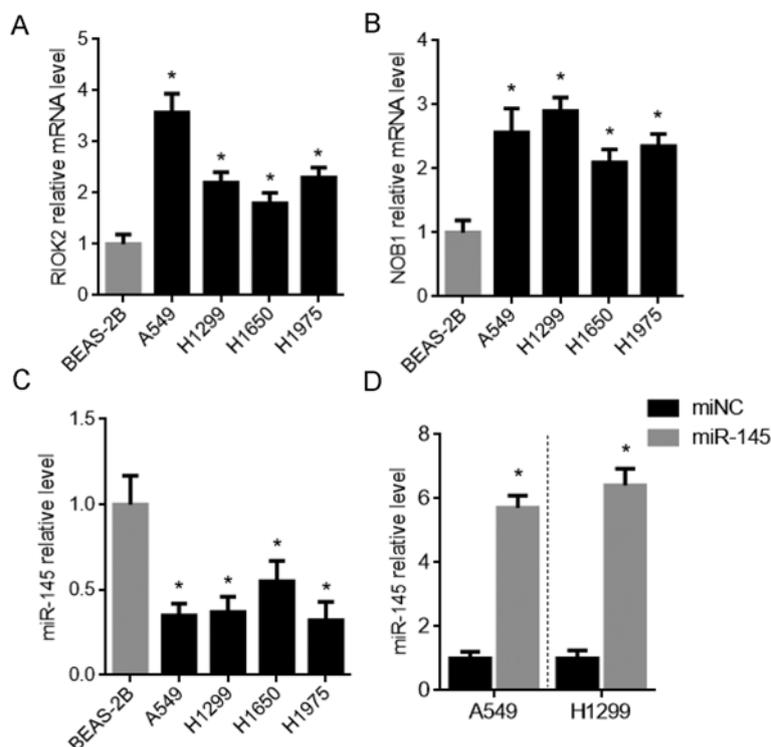
Figure 4. Expression levels of RIOK2, NOB1 and miR-145 in NSCLC cells, as detected by reverse transcription-quantitative polymerase chain reaction. mRNA expression levels of (A) RIOK2 and (B) NOB1 in NSCLC cells. (C) Expression levels of miR-145 in NSCLC cells. *P<0.05, compared with the normal lung cell line BEAS-2B. (D) Expression levels of miR-145 in A549 and H1299 cells post-transfection with miR-145 mimics. *P<0.05, compared with miNC-transfected cells. miR-145, microRNA-145; miNC, microRNA negative control; NOB1, nin one binding protein; NSCLC, non-small cell lung cancer; RIOK2, right open reading frame kinase 2.

NOB1-3'UTR, a marked decrease was observed in luciferase activity, as compared with in cells cotransfected with miNC and mt-RIOK2 or NOB1-3'UTR (P<0.05, Fig. 3B and C).

*Expression of RIOK2, NOB1 and miR-145 in NSCLC cells.* The expression levels of RIOK2, NOB1 and miR-145 were detected in various NSCLC cell lines by RT-qPCR. The results demonstrated that the mRNA expression levels of RIOK2 and NOB1 were increased in NSCLC cells (A549, H1299, H1975 and H1650) compared with in the normal human lung cell line BEAS-2B (P<0.05; Fig. 4A and B). In addition, the expression levels of miR-145 were decreased in NSCLC cells (A549, H1299, H1975 and H1650) compared with in the normal human lung cell line BEAS-2B (P<0.05; Fig. 4C). A549 and H1299 cells were selected as an NSCLC cell model for subsequent functional assays. Post-transfection of cells with miR-145 mimics, miR-145 expression was markedly increased compared with in the miNC-transfected cells (P<0.05; Fig. 4D).

*Effects of miR-145 mimics and siRNAs against RIOK2 and NOB1 expression on NSCLC cells.* The expression levels of RIOK2 and NOB1 were detected following transfection of NSCLC cells with miR-145 mimics, siRIOK2 and siNOB1 using western blotting. The results demonstrated that the protein expression levels of RIOK2 and NOB1 were inhibited by miR-145 overexpression in A549 and H1299 NSCLC cells compared with in miNC-transfected cells (P<0.05; Fig. 5A). Furthermore, RIOK2 protein expression was significantly

inhibited by siRIOK2, whereas NOB1 protein expression was significantly inhibited by siNOB1, as compared with in the siNC-transfected groups (P<0.05; Fig. 5B).

*Inhibitory effects of miR-145 on NSCLC cell growth may be mediated by RIOK2 and NOB1.* An MTT assay was used to investigate the inhibitory effects of miR-145 or siRNAs on NSCLC cell growth. miR-145 markedly inhibited the growth of A549 and H1299 cells at 72 and 96 h compared with the miNC-transfected cells (P<0.05; Fig. 6A and B). In addition, cell growth was reduced in cells transfected with siRNAs that target RIOK2 or NOB1 compared with in siNC-transfected cells (P<0.05; Fig. 6C and D).

*Inhibitory effects of miR-145 on NSCLC cell invasion and migration may be mediated by RIOK2 and NOB1.* Transwell assays were used to evaluate the effects of miR-145-mediated RIOK2 and NOB1 inhibition on NSCLC cell migration and invasion. miR-145 transfection significantly decreased A549 and H1299 cell migration and invasion compared with in miNC-transfected cells (P<0.05; Figs. 7 and 8).

## Discussion

Human NSCLC is the leading cause of cancer-associated mortality in patients worldwide (23). However, the molecular mechanism underlying NSCLC occurrence and development remains unclear (24), and NSCLC is thought to be caused by numerous complex factors, including the aberrant expression of
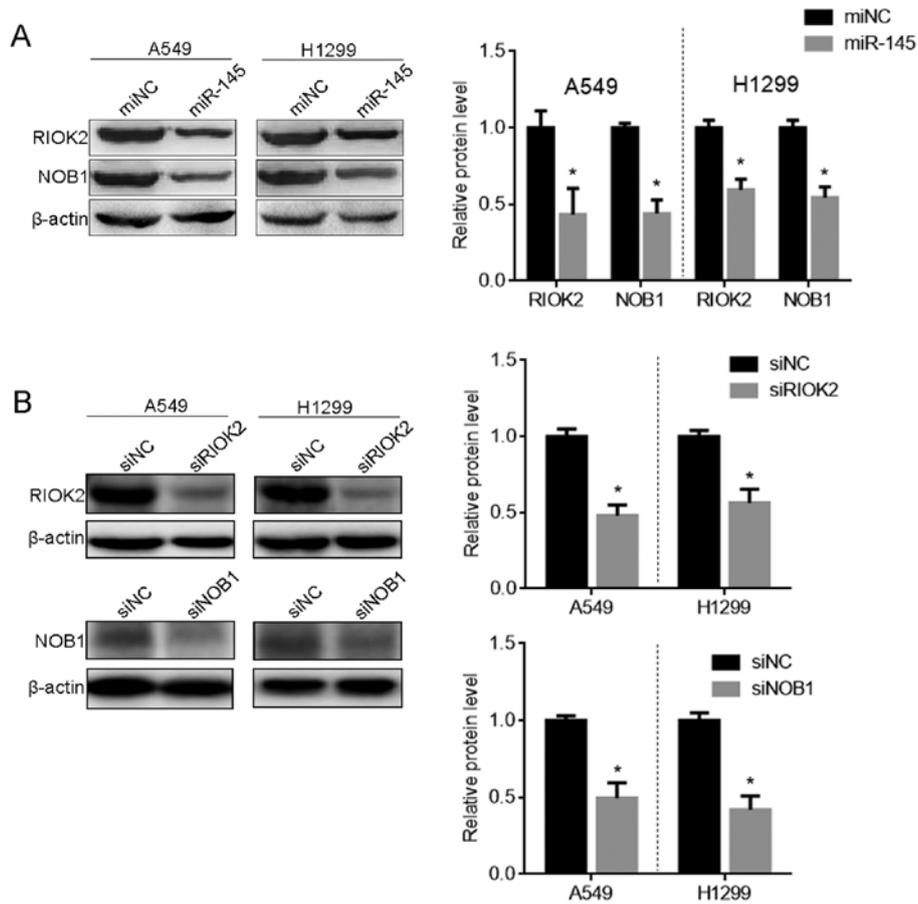
Figure 5. RIOK2 and NOB1 expression is inhibited by miR-145 mimics or siRNAs in A549 and H1299 NSCLC cells, as detected by western blotting. (A) RIOK2 and NOB1 protein expression was inhibited by miR-145 mimics in A549 and H1299 NSCLC cells. *P<0.05, compared with miNC-transfected cells. (B) RIOK2 and NOB1 protein expression was inhibited by siRIOK2 and siNOB1 in A549 and H1299 NSCLC cells, respectively. *P<0.05, compared with siNC-transfected cells. miR-145, microRNA-145; miNC, microRNA negative control; NOB1, nin one binding protein; NSCLC, non-small cell lung cancer; RIOK2, right open reading frame kinase 2; si, small interfering RNA.
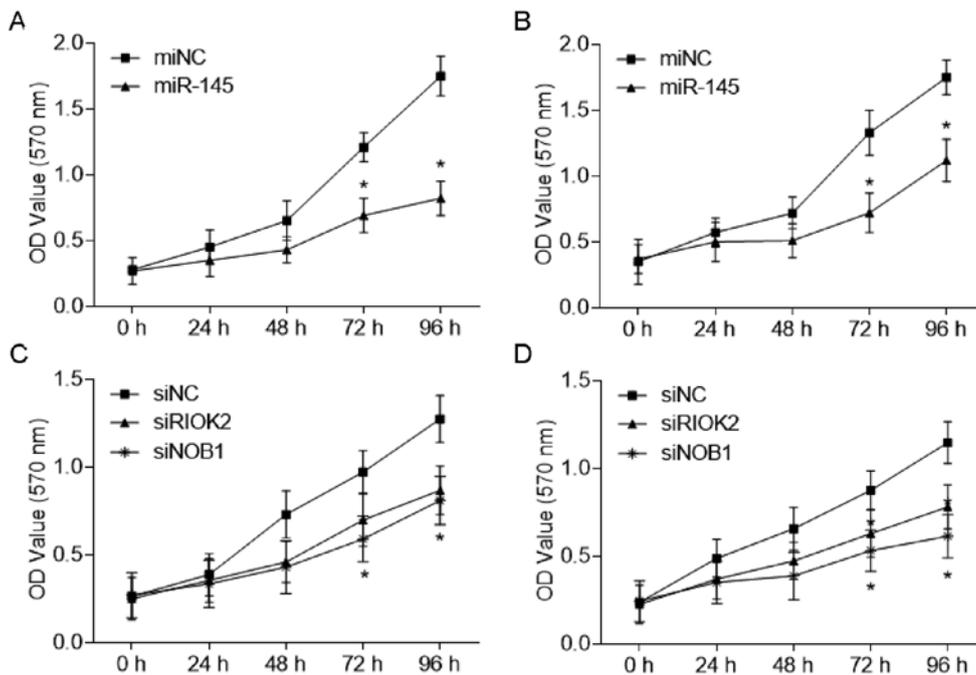


Figure 6. Effects of miR-145 or siRNAs on non-small cell lung cancer cell growth. Growth of (A) A549 and (B) H1299 cells was inhibited by miR-145 mimics. *P<0.05, compared with miNC-transfected cells. Growth of (C) A549 and (D) H1299 cells was inhibited by siRNAs. *P<0.05, compared with siNC-transfected cells. miR-145, microRNA-145; miNC, microRNA negative control; NOB1, nin one binding protein; OD, optical density; RIOK2, right open reading frame kinase 2; si, small interfering RNA.
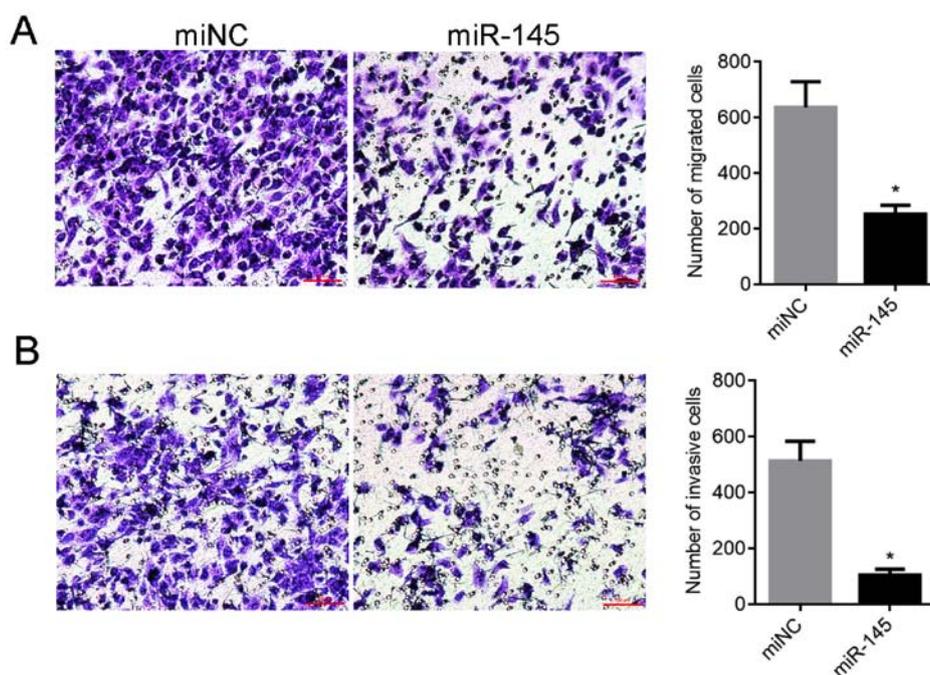
Figure 7. Effects of miR-145 transfection on the invasion and migration of A549 non-small cell lung cancer cells. miR-145 transfection inhibited the (A) migratory and (B)invasive abilities of A549 cells. Magnification, x200. *P<0.05, compared with miNC-transfected cells. miR-145, microRNA-145; miNC, miRNA negative control.
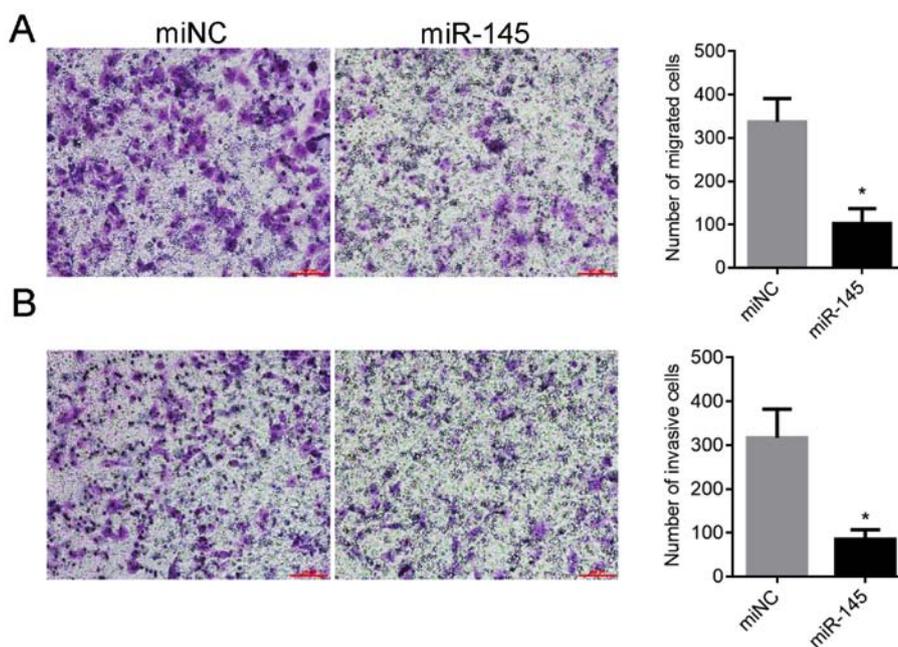


Figure 8. Effects of miR-145 transfection on the invasion and migration of H1299 non-small cell lung cancer cells. miR-145 transfection inhibited the (A) migratory and (B) invasive abilities of H1299 cells. Magnification, x200. *P<0.05, compared with miNC-transfected cells. miR-145, microRNA-145; miNC, miRNA negative control.

various tumor suppressor genes (25). The human NOB1 gene, which comprises nine exons and eight introns, is located on human chromosome 16q22.1; NOB1 encodes a 50-kDa protein, which comprises a PilT amino terminus domain and a zinc ribbon domain, and is predominantly expressed in the liver, lung and spleen (26). NOB1 functions as an oncogene, which is overexpressed and has important roles in various types of human cancer, including ovarian cancer (27), hepatocellular carcinoma (28), breast cancer (29), glioma (30), thyroid carcinoma (31) and prostate cancer (32). In our previous study, it was revealed that NOB1 is highly expressed in NSCLC (3), and its expression in patients with NSCLC may be significantly correlated with clinical parameters, including TNM stage, lymph node metastasis and histopathological grade, thus suggesting it may be a biomarker of NSCLC. RIOK2 is a member of the RIO family (5), which is highly expressed in various tumor

types (33). Our previous study demonstrated that RIOK2 is also increased in NSCLC tissues and its expression is positively correlated with NOB1 (4,8). Therefore, RIOK2 and NOB1 may be considered potential targets for NSCLC therapy.

In recent years, miRNAs have been suggested for use as clinical therapeutic agents for the treatment of human cancer (34,35). Notably, miRNAs are able to directly suppress gene expression with low toxicity and few side effects. In the present study, the expression levels of the tumor suppressor miRNA, miR-145, were decreased in NSCLC tumor tissues, whereas RIOK2 and NOB1 were increased in NSCLC tumor tissues. Furthermore miR-145 expression was negatively correlated with RIOK2 and NOB1. The 3'UTR regions of RIOK2 and NOB1 mRNA were reported to contain miR-145-binding sites according to online software, and the inhibitory activities of miR-145 against these genes were validated by a DLR assay. Furthermore, in NSCLC cells (A549, H1299, H1975 and H1650), the expression profiles of RIOK2, NOB1 and miR-145 were similar to those in NSCLC tumor tissues, particularly in A549 and H1299 cells compared with in the normal lung cell line BEAS-2B. Subsequently, post-transfection with miR-145 mimics, the endogenous expression of miR-145 was increased in A549 and H1299 cells, whereas the expression levels of RIOK2 and NOB1 were markedly inhibited. These results indicated that miR-145 may possess therapeutic potential, and may be able to decrease RIOK1 and NOB1 expression in patients with NSCLC. NOB1 is an endonuclease that catalyzes the processing of 20S pre-rRNA to mature 18S rRNA, and regulates ribosome assembly (36). RIOK2 is located at the center of the pre-ribosomal particle, interacts with numerous assembly factors, including NOB1, and directly binds to ribosomal protein (Rps)5, Rps14 and Rps15, which is required for 20S cleavage. Notably, RIOK2 acts as a master-regulator of the NOB1-dependent 20S cleavage step. NOB1 can interact with Rps5 and Rps14, both of which are required for the 20S pre-rRNA cleavage step (37,38). The interaction between RIOK2 and NOB1 was previously confirmed by a reverse pull-down assay (39). Ribosomal proteins serve important roles in cell cycle progression (6), and the inhibition of NSCLC cell viability, migration and invasion may be induced via modulation of cell cycle progression induced by RIOK2 and NOB1 downregulation. The present study confirmed that the viability, migration and invasion of A549 and H1299 NSCLC cells were markedly inhibited post-transfection with miR-145 mimics; these effects may be mediated by miR-145-induced inhibition of RIOK2 and NOB1.

In conclusion, the present study suggested that RIOK2 and NOB1 may be considered biomarkers in NSCLC, and may be potential targets for clinical NSCLC therapy. Furthermore, miR-145 may possess therapeutic potential, due to its ability to inhibit both genes.

## Acknowledgements

Not applicable.

## Funding

## Availability of data and materials

All data generated or analyzed during this study are included in this published article.

## Authors' contributions

KL and MG designed the study; SW, SZ, KY, WL and MG performed the experiments; HC and QYo analyzed the data; QYe collected the tissue samples and analyzed the tissue results; FW provided technical guidance in experiments, performed cell culture, and was involved in drafting the manuscript and revising it critically for important intellectual content; KL, MG, QYo, QYe and FW provided helpful discussions and critically reviewed the manuscript; KL and MG supervised the study; KL wrote the manuscript. All authors have read and approved the final version of the manuscript.

## Ethics approval and consent to participate

The present study was approved by the Ethics Committee of the Affiliated Hospital of Nantong University (Nantong, China). Written informed consent was obtained from each patient.

## Consent for publication

Not applicable.

## Competing interests

The authors declare that they have no competing interests.

## References

1. Molina JR, Yang P, Cassivi SD, Schild SE and Adjei AA: Non-small cell lung cancer: Epidemiology, risk factors, treatment, and survivorship. Mayo Clin Proc 83: 584-594, 2008.
2. Lamanna AC and Karbstein K: Nob1 binds the single-stranded cleavage site D at the 3'-end of 18S rRNA with its PIN domain. Proc Natl Acad Sci USA 106: 14259-14264, 2009.
3. Liu K, Chen HL, Gu MM and You QS: Relationship between NOB1 expression and prognosis of resected non-small cell lung cancer. Int J Biol Markers 30: e43-e48, 2015.
4. Liu K, Gu MM, Chen HL and You QS: NOB1 in non-small-cell lung cancer: Expression profile and clinical significance. Pathol Oncol Res 20: 461-466, 2014.
5. Kiburu IN and LaRonde-LeBlanc N: Interaction of Rio1 kinase with toyocamycin reveals a conformational switch that controls oligomeric state and catalytic activity. PLoS One 7: e37371, 2012.
6. Darnell JC: Molecular biology. Ribosome rescue and neurodegeneration. Science 345: 378-379, 2014.
7. Turowski TW, Lebaron S, Zhang E, Peil L, Dudnakova T, Petfalski E, Granneman S, Rappsilber J and Tollervey D: Rio1 mediates ATP-dependent final maturation of 40S ribosomal subunits. Nucleic Acids Res 42: 12189-12199, 2014.

8. Liu K, Chen HL, Wang S, Gu MM, Chen XM, Zhang SL, Yu KJ and You QS: High Expression of RIOK2 and NOB1 Predict human non-small cell lung cancer outcomes. Sci Rep 6: 28666, 2016.

9. Ambros V: The functions of animal microRNAs. Nature 431: 350-355, 2004.

10. Bartel DP: MicroRNAs: Genomics, biogenesis, mechanism, and function. Cell 116: 281-297, 2004.

11. Shenouda SK and Alahari SK: MicroRNA function in cancer: Oncogene or a tumor suppressor? Cancer Metastasis Rev 28: 369-378, 2009.

12. Gao Y, Zhang Z, Li K, Gong L, Yang Q, Huang X, Hong C, Ding M and Yang H: Linc-DYNC2H1-4 promotes EMT and CSC phenotypes by acting as a sponge of miR-145 in pancreatic cancer cells. Cell Death Dis 8: e2924, 2017.

13. Goto Y, Kurozumi A, Arai T, Nohata N, Kojima S, Okato A, Kato M, Yamazaki K, Ishida Y, Naya Y, et al: Impact of novel miR-145-3p regulatory networks on survival in patients with castration-resistant prostate cancer. Br J Cancer 117: 409-420, 2017.

14. Wei H, Wen-Ming C and Jun-Bo J: Plasma miR-145 as a novel biomarker for the diagnosis and radiosensitivity prediction of human cervical cancer. J Int Med Res 45: 1054-1060, 2017.

15. Hu CE, Du PZ, Zhang HD and Huang GJ: Long noncoding RNA CRNDE promotes proliferation of gastric cancer cells by targeting miR-145. Cell Physiol Biochem 42: 13-21, 2017.

16. Moon S, Kim DK and Kim J: Apoptosis-related microRNA-145-5p enhances the effects of pheophorbide a-based photodynamic therapy in oral cancer. Oncotarget 8: 35184-35192, 2017.

17. Sheng N, Tan G, You W, Chen H, Gong J, Chen D, Zhang H and Wang Z: miR-145 inhibits human colorectal cancer cell migration and invasion via PAK4-dependent pathway. Cancer Med 6: 1331-1340, 2017.

18. Ding Y, Zhang C, Zhang J, Zhang N, Li T, Fang J, Zhang Y, Zuo F, Tao Z, Tang S, et al: miR-145 inhibits proliferation and migration of breast cancer cells by directly or indirectly regulating TGF-β1 expression. Int J Oncol 50: 1701-1710, 2017.

19. Minami K, Taniguchi K, Sugito N, Kuranaga Y, Inamoto T, Takahara K, Takai T, Yoshikawa Y, Kiyama S, Akao Y, et al: miR-145 negatively regulates Warburg effect by silencing KLF4 and PTBP1 in bladder cancer cells. Oncotarget 8: 33064-33077, 2017.

20. Liu S, Gao G, Yan D, Chen X, Yao X, Guo S, Li G and Zhao Y: Effects of miR-145-5p through NRAS on the cell proliferation, apoptosis, migration, and invasion in melanoma by inhibiting MAPK and PI3K/AKT pathways. Cancer Med 6: 819-833, 2017.

21. Chen C, Ridzon DA, Broomer AJ, Zhou Z, Lee DH, Nguyen JT, Barbisin M, Xu NL, Mahuvakar VR, Andersen MR, et al: Real-time quantification of microRNAs by stem-loop RT-PCR. Nucleic Acids Res 33: e179, 2005.

22. Livak KJ and Schmittgen TD: Analysis of relative gene expression data using real-time quantitative PCR and the 2(-Delta Delta C(T)) Method. Methods 25: 402-408, 2001.

23. Torre LA, Bray F, Siegel RL, Ferlay J, Lortet-Tieulent J and Jemal A: Global cancer statistics, 2012. CA Cancer J Clin 65: 87-108, 2015.

24. Ansari J, Shackelford RE and El-Osta H: Epigenetics in non-small cell lung cancer: From basics to therapeutics. Transl Lung Cancer Res 5: 155-171, 2016.

25. Reid G, Kao SC, Pavlakis N, Brahmbhatt H, MacDiarmid J, Clarke S, Boyer M and van Zandwijk N: Clinical development of TargomiRs, a miRNA mimic-based treatment for patients with recurrent thoracic cancer. Epigenomics 8: 1079-1085, 2016.

26. Zhang Y, Ni J, Zhou G, Yuan J, Ren W, Shan Y, Tang W, Yu L and Zhao S: Cloning, expression and characterization of the human NOB1 gene. Mol Biol Rep 32: 185-189, 2005.

27. Lin Y, Peng S, Yu H, Teng H and Cui M: RNAi-mediated down-regulation of NOB1 suppresses the growth and colony-formation ability of human ovarian cancer cells. Med Oncol 29: 311-317, 2012.

28. Lu Z, Guo Q, Shi A, Xie F and Lu Q: Downregulation of NIN/RPN12 binding protein inhibit the growth of human hepato-cellular carcinoma cells. Mol Biol Rep 39: 501-507, 2012.

29. Li XY, Luo QF, Li J, Wei CK, Kong XJ, Zhang JF and Fang L: Clinical significance of NOB1 expression in breast infiltrating ductal carcinoma. Int J Clin Exp Pathol 6: 2137-2144, 2013.

30. Wang H, Li P and Zhao B: Knockdown of NOB1 expression by RNAi inhibits cellular proliferation and migration in human gliomas. Gene 528: 146-153, 2013.

31. Lin S, Meng W, Zhang W, Liu J, Wang P, Xue S and Chen G: Expression of the NOB1 gene and its clinical significance in papillary thyroid carcinoma. J Int Med Res 41: 568-572, 2013.

32. Liu G, Shen D, Jiao L and Sun Y: Nin one binding protein expression as a prognostic marker in prostate carcinoma. Clin Transl Oncol 16: 843-847, 2014.

33. Weinberg F, Reischmann N, Fauth L, Taromi S, Mastroianni J, Köhler M, Halbach S, Becker AC, Deng N, Schmitz T, et al: The atypical kinase RIOK1 promotes tumor growth and invasive behavior. EBioMedicine 20: 79-97, 2017.

34. Dolly SO, Collins DC, Sundar R, Popat S and Yap TA: Advances in the development of molecularly targeted agents in non-Small-cell lung cancer. Drugs 77: 813-827, 2017.

35. Meerson A, Traurig M, Ossowski V, Fleming JM, Mullins M and Baier LJ: Human adipose microRNA-221 is upregulated in obesity and affects fat metabolism downstream of leptin and TNF-α. Diabetologia 56: 1971-1979, 2013.

36. Pertschy B, Schneider C, Gnädig M, Schäfer T, Tollervey D and Hurt E: RNA helicase Prp43 and its co-factor Pfa1 promote 20 to 18 S rRNA processing catalyzed by the endonuclease Nob1. J Biol Chem 284: 35079-35091, 2009.

37. Ferreira-Cerca S, Sagar V, Schäfer T, Diop M, Wesseling AM, Lu H, Chai E, Hurt E and LaRonde-LeBlanc N: ATPase-dependent role of the atypical kinase Rio2 on the evolving pre-40S ribosomal subunit. Nat Struct Mol Biol 19: 1316-1323, 2012.

38. Woolls HA, Lamanna AC and Karbstein K: Roles of Dim2 in ribosome assembly. J Biol Chem 286: 2578-2586, 2011.

39. Campbell MG and Karbstein K: Protein-protein interactions within late pre-40S ribosomes. PLoS One 6: e16194, 2011.